The Predischarge Chromophore in Bacteriorhodopsin: A ^{15}N Solid-State NMR Study of the L Photointermediate†

Jingui G. Hu,‡,§ Boqin Q. Sun,‡,§ Aneta T. Petkova,‡,§ Robert G. Griffin,§ and Judith Herzfeld*,‡

Department of Chemistry and Keck Institute for Cellular Visualization, Brandeis University, Waltham, Massachusetts 02254, and Department of Chemistry and Francis Bitter Magnet Laboratory, Massachusetts Institute of Technology, Cambridge, Massachusetts 02139

Received February 24, 1997; Revised Manuscript Received May 29, 1997⊗

ABSTRACT: The L_{550} intermediate in the bacteriorhodopsin (bR) photocycle has drawn much attention with respect to the mechanism of light-driven proton transport because it selectively releases the Schiff base (SB) proton to the extracellular proton channel in the L→M transition. Here we extend our solid-state NMR studies of bR photocycle intermediates to the L state. Under conditions that stabilize L_{550}, a new SB signal is detected in the ^{15}N NMR spectrum which disappears upon thermal relaxation. This signal is in the range for a protonated SB, but downfield from the SB signals of bR_{568} and N_{520}. Since steric interactions would have the opposite effect on shielding, the data argue against a 13,14-*dicis* chromophore in L_{550}. Comparison with the ^{15}N chemical shifts of halide salts of protonated Schiff bases (pSB's) of retinal suggests that the interaction of the SB with its counterion is significantly stronger in L_{550} than in N_{520} (which in turn is stronger than in bR_{568}). This is consistent with models of the early photocycle in which the electrostatic interaction between the SB and its counterion constitutes an important constraint. Although the L counterion interaction is comparable to that of a 6-*s-trans*,13-*cis* chloride salt, the visible spectrum is strongly red-shifted from the $\lambda_{max} = 491$ nm of the chloride. This suggests some double bond strain in L_{550}, particularly about the C=N bond. This strain is apparently gone in the N intermediate, which has a normal relationship between the ^{15}N chemical shift and λ_{max}. Such a relaxed chromophore is consistent with orientation of the SB proton toward the cytoplasmic surface in the N intermediate.

Bacteriorhodopsin (bR)[1] is the sole protein in the purple patches of the plasma membranes of *Halobacterium salinarium* (also known as *Halobacterium halobium*) (Oesterhelt & Stoeckenius, 1971, 1973a). The 26 kDa polypeptide chain of 248 amino acids (Khorana et al., 1979; Ovchinnikov et al., 1979) forms a bundle of 7 transmembrane α-helices (Henderson et al., 1990), which encapsulates a retinal chromophore connected to the protein via a protonated Schiff base (pSB) linkage with Lys216. The counterion of the pSB is likely to be a hydrogen-bonded complex comprising water (de Groot et al., 1990), Asp85, Asp212, and Arg82 (Braiman et al., 1988; Gerwert et al., 1989; Henderson et al., 1990).

In the resting state and in the dark, bR contains two isomers, bR_{568} and bR_{555}, with 6-*s-trans*,*all-trans*,15-*anti*- and 6-*s-trans*,13-*cis*,15-*syn*-retinal structures, respectively (Harbison et al., 1985, 1984; Pettei et al., 1977). The bR_{555} photocycle branches to bR_{568}, so light-adapted bR is pure bR_{568}. Only the bR_{568} photocycle results in proton transport (Oesterhelt & Stoeckenius, 1973b). The proton-motive cycle is initiated by the photoinduced transition from the 6-*s-trans*,*all-trans*,15-*anti* bR_{568} state to the 6-*s-trans*,13-*cis*,15-*anti* J_{625} intermediate (Fodor et al., 1988). The cycle is completed by thermal steps through a series of other intermediates, K_{590}, L_{550}, M_{412}, N_{520}, and O_{640} (Figure 1). In each photocycle, a proton is released at the extracellular surface and replaced from the cytoplasmic side, resulting in net pumping. At the SB, the proton release and uptake processes happen in the reactions L→M(I) and M(II)→N, respectively (see Figure 1).

The photocycle has been most extensively characterized according to the color changes corresponding to the different λ_{max}'s noted in the subscript for each photointermediate. Our recent work on a series of 6-*s-trans*,*all-trans*,15-*anti* pSB's (Hu et al., 1994) and a series of 6-s-*trans*,*13-cis*,15-*anti* pSB's (Hu et al., 1997) indicates that the spectral tuning in bR_{568}, bR_{555}, and N_{520} can be completely explained by the synergistic effects of the strength of the electrostatic interaction between the pSB and its counterion, and the isomerization of the linkage between the ionone ring and the polyene chain of the retinal upon insertion into the binding pocket.

The nature of the L intermediate is critical for bR function because it leads to vectorial release of the SB proton in the L→M transition. Comparison of L with N will be helpful in understanding the gating of proton movement because the

† This research was supported by the National Institutes of Health (GM-36810, GM-23289, and RR-00993).

* Corresponding author (telephone, 617-736-2538; FAX, 617-736-2516; E-mail, herzfeld@binah.cc.brandeis.edu).

‡ Brandeis University.

§ Massachusetts Institute of Technology.

⊗ Abstract published in *Advance ACS Abstracts,* August 1, 1997.

[1] Abbreviations: bR, bacteriorhodopsin; bR_{568} or LA, *all-trans*,15-*anti* component of dark-adapted bacteriorhodopsin and sole component of light-adapted bacteriorhodopsin; bR_{555}, 13-*cis*,15-*syn* component of dark-adapted bacteriorhodopsin; CP, cross-polarization; DA, dark-adapted resting state of bR, an ∼1:2 mixture of bR_{568} and bR_{555}; J or J_{625}, primary photoproduct of bR_{568}; K or K_{590}, relaxation product of J and the precursor of L; L or L_{550}, protonated photointermediate preceding M_{412} in the bR photocycle; M or M_{412}, deprotonated photointermediate in the photocycle of bR; N or N_{520}, protonated photointermediate following M_{412} in the photocycle of bR; Lys, lysine; MAS, magic angle spinning; NMR, nuclear magnetic resonance; pSB, protonated Schiff base; SB, Schiff base; SSNMR, solid-state NMR.

S0006-2960(97)00416-9 CCC: $14.00

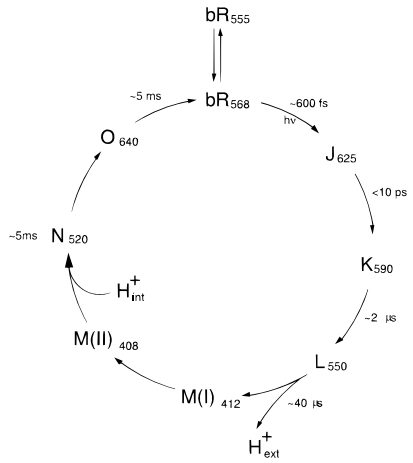

FIGURE 1: Photocycle of bR_{568} showing the relationships among the functionally important intermediates. Subscripts indicate the wavelengths of maximum visible absorbance. The retinal Schiff base is protonated in all but the M states, and the retinal polyene chain is 13-*cis* in all but the O_{640} and bR_{568} states where it is *all-trans*.

SB proton in L is discharged to the extracellular side while the SB proton in N is taken from the intracellular side. Two extreme models have been proposed for this gating. In one, the changes in SB connectivity between the L and N intermediates are due entirely to isomerization of the chromophore. In particular, it has been proposed that a 13,-14-*dicis* conformation (Orlandi & Schulten, 1979; Schulten, 1978; Schulten et al., 1984; Schulten & Tavan, 1978) in L (which would have the SB proton pointing toward the extracellular surface) relaxes to a 13-*cis* conformation in N (which would have the SB proton pointing toward the intracellular surface). Isomerization from 13,14-*dicis* to 13-*cis* by rotation about the 14−15 single bond is postulated to occur in the M intermediate, in concert with, and stimulated by, Schiff base proton transfer to Asp85 (Zhou et al., 1993). The opposing model of gating is predicated on essentially identical, 13-*cis* chromophore conformations in the L, M and N photointermediates (Fodor et al., 1988). In this case, rearrangement of the surrounding protein is required to control proton movement. The protein structure is proposed to change between two geometries, T and C, suited to accommodate *all-trans*- and 13-*cis*-retinal, respectively. This protein conformational change is proposed to serve as the switch for the connectivity of the retinal Schiff base.

Recent experimental results (Fischer et al., 1994; Henderson et al., 1990; Mathies & Li, 1995; Mathies et al., 1991; Nilsson et al., 1995; Sonart et al., 1994; Subramaniam et al., 1993; Weidlich et al., 1995; Weidlich & Siebert, 1993) and theoretical modeling (Engels et al., 1995; Humphrey et al., 1995; Scharnagl et al., 1994, 1995; Zhou et al., 1993) suggest a hybrid mechanism, including unwinding of a twisted 13-*cis* chromophore and remodeling of the proton transport pathway. However, the correct structure for the chromophore in the L state and its role in proton pumping remain to be established by further experiments. To date, solid-state NMR (SSNMR) has been proved to be the most unambiguous method for determining the detailed chromophore structure in bR (de Groot et al., 1989; Farrar et al., 1993; Harbison et al., 1983; Hu et al., 1995; Lakshmi et al., 1993). Unfortunately, the L intermediate has heretofore been inaccessible for SSNMR. This work describes our first SSNMR studies on the L intermediate at very low temperatures (down to −130 °C) utilizing ^{15}N MAS NMR. We find evidence for a stronger SB−counterion interaction in L_{550} than in any of the other bR states studied previously. That the L state is nevertheless strongly red-shifted suggests double bond strain in the chromophore, especially around the C═N bond.

MATERIALS AND METHODS

The ^{15}N NMR signal of the SB in [ϵ-^{15}N]Lys-bR is a good indicator for the various photointermediates of bR, because the SB is the active site in proton pumping and the ^{15}N chemical shift is sensitive to changes in the interactions of the pSB. For the bR states prepared previously, including DA, bR_{568}, M, and N, the SB ^{15}N signals are well resolved. It seems likely that the signal of L will be separated from these intermediates, since its structure is presumably different.

Preparation of [ϵ-^{15}N]Lys-bR. bR was selectively labeled by growing *Halobacterium salinarium* strain (JW-3) in a synthetic medium containing L-[ϵ-^{15}N]lysine (Argade et al., 1981). The incorporation of the labeled lysine into bR was measured by the coincorporation of trace L-[ϵ-$^{3}H_2$]lysine. The results indicate no scrambling of the radioactive label to other amino acid residues in the protein. The isolation of the purple membranes was achieved by the method of Oesterhelt and Stoeckenius (1974). Prior to spectroscopy, the sample was washed several times with a 0.1 M solution of NaCl at pH 10.0 or pH 7.0, depending on the desired conditions. The bR suspension was centrifuged at 30000*g* for 1 h following each wash, and the bR pellet from the final spin was packed into a transparent single-crystal sapphire rotor (7 mm in outside diameter) which was tightly sealed with transparent Kel-F endcaps (DOTY Scientific, Columbia, SC).

In Situ Illumination of the bR Sample. Light to initiate the bR photocycle was delivered from a 1000 W xenon lamp to the sample via a glass optic fiber bundle. Careful alignment of the fiber at both ends is required for efficient illumination. The selection of light frequencies for the preparation of different photointermediates was achieved by inserting glass filters between the fiber and the light source. A water filter was used to eliminate the heat caused by near-IR components. With this setup, different photointermediates could be prepared by simply changing the trapping temperature and the illumination frequencies.

Light-Adaptation of bR. The dark-adapted bR (DA), containing bR_{568} and bR_{555}, was converted to light-adapted bR (LA), comprising only bR_{568}, by illumination with white light at 0 °C for a few hours.

Preparation of L_{550}. L_{550} was trapped by illuminating LA with $\lambda > 610$ nm in the temperature range of −95 to −130 °C for at least 2 h.

Preparation of M_{412}. M_{412} was trapped by illuminating LA with $\lambda > 540$ nm at −60 °C for an hour.

Preparation of N_{520}. N_{520} was trapped by illuminating LA with $\lambda > 540$ nm at around −20 °C for about an hour.

^{15}N Solid-State NMR. Routine CP/MAS spectra were acquired on a custom-designed spectrometer operating at a field of 7.4 T (317.6 MHz, 79.9 MHz, and 32.2 MHz for ^{1}H, ^{13}C, and ^{15}N, respectively). Generally, the lower the temperature during data acquisition, the better the S/N of the NMR spectra. However, the choice of temperature is limited by the capabilities of the NMR probe and other

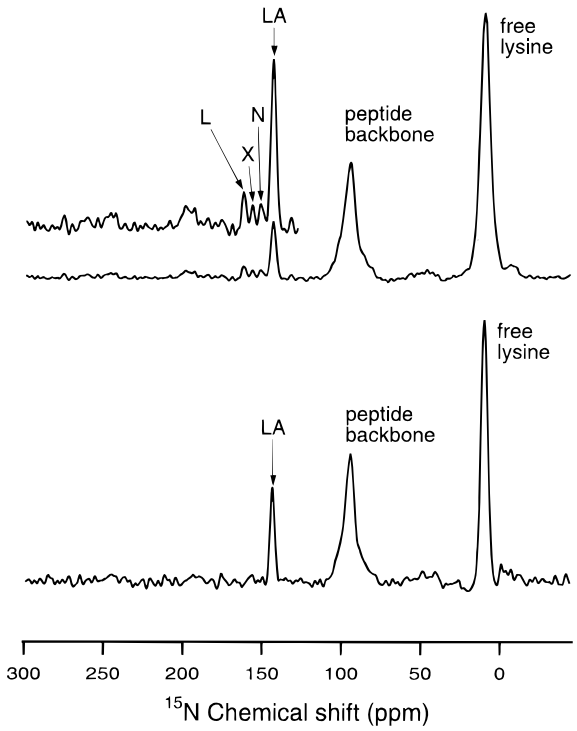

FIGURE 2: ^{15}N CP/MAS spectra of [ϵ-^{15}N]Lys-bR in 0.1 M NaCl at pH 7.0 taken at −125 °C. Top: Spectrum obtained after illumination of LA with wavelengths >610 nm for several hours at −125 °C. The inset is expanded 3-fold. Bottom: The same sample after relaxation in the dark at −80 °C.

accessories, and by the stability of the photointermediate(s) of interest. Sample temperatures were determined in separate experiments by observing the position of the ^{207}Pb resonance in $Pb(NO_3)_2$ and the reading of an external thermocouple. Typical conditions for SSNMR data acquisition were as follows: proton 90° pulse 3.5 μs, CP mixing time 2 ms, FID sampling 1024 points, recycling delay 3 s, dwell time 20 μs, sample spinning speed 3−4 kHz, and continuous proton decoupling during data acquisition. A double resonance probe with variable temperature control was used. ^{15}N chemical shifts are reported relative to saturated (5.6 M) aqueous $^{15}NH_4Cl$.

RESULTS

pH 7.0. It has been reported that the L photointermediate is stabilized at −103 °C in NaCl at pH 7.0 (Kandori et al., 1995). Illumination of LA under these conditions with λ > 540 nm produces several new ^{15}N SB signals (results not shown). With light of longer wavelengths, all the new signals decline in intensity except the one at 161 ppm. We therefore tentatively assign the latter to L and the former to photoproducts of L or N. Light restricted to λ > 610 nm results in a relatively clean spectrum (top, Figure 2) showing only one signal, at 157 ppm, not attributable to LA, L, or N. We temporarily designate this photoproduct as X. All the observed species relax to LA at −80 °C in the dark (bottom, Figure 2), consistent with the thermal instability of photointermediates of bR at pH 7.0.

pH 10.0. Similar experiments were performed under identical conditions but at pH 10.0. At this pH, both M_{412} and N_{520} are stable at relatively high temperatures. Therefore, L trapped at low temperatures should relax to M and N upon warming to appropriately chosen temperatures.

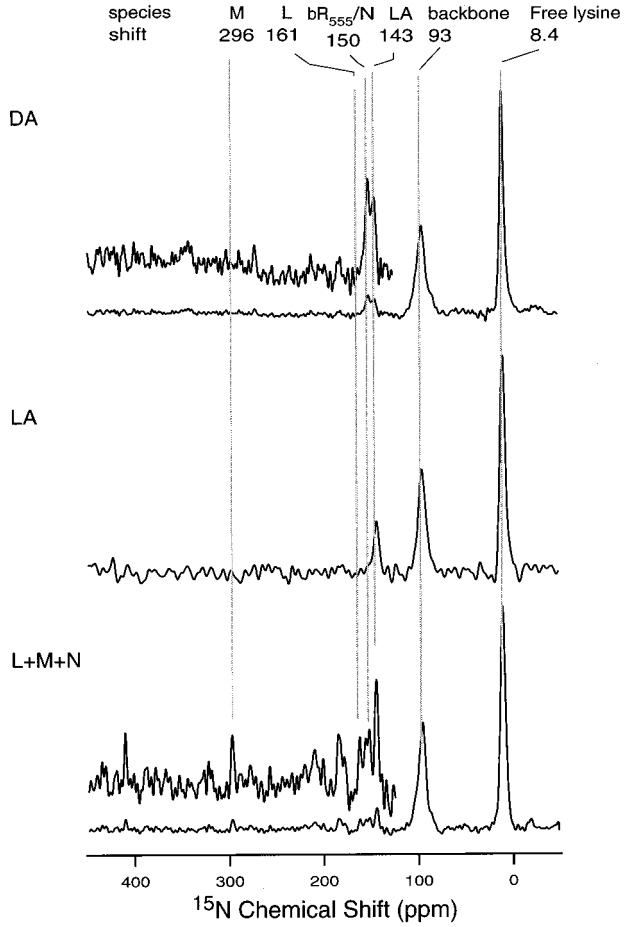

FIGURE 3: ^{15}N CP/MAS spectra of [ϵ-^{15}N]Lys-bR in 0.1 M NaCl at pH 10.0 taken at −110 °C. Top: A doublet at around 150 ppm originates from the SB in the two isomers in DA. Middle: After light adaptation, bR_{555} is converted to bR_{568} completely, as indicated by the singlet from the SB at 143 ppm. Bottom: Illumination at −100 °C with wavelengths > 610 nm drives LA to a mixture of L, M, and N.

Figure 3 shows the conversion of DA to LA and the results of illuminating LA with λ > 610 nm at −100 °C. As at pH 7.0, L and X signals occur at 161 and 157 ppm, respectively. However, this time they coexist with M_{412} [downfield at 296 ppm (Lakshmi et al., 1994), with the large CSA characteristic of a deprotonated SB (Harbison et al., 1983)], as well as N_{520} [at 150 ppm (Lakshmi et al., 1994)] and unconverted LA [at 143 ppm (de Groot et al., 1989)]. The L signal at −100 °C accounts for about 20% of the total bR. The trapping temperature only affects the relative concentrations of the intermediates.

In order to confirm that the 161 ppm signal belongs to L, we examined its thermal stability and its thermal relaxation products. As expected, the signal completely disappears in the dark at −75 °C (Figure 4) (comparable to −80 °C for pH 7.0 in Figure 2). At the same time, the intensity of the M_{412} intermediate increases because it is stable under these conditions (temperature, pH value, and salt concentration). Thus, the 161 ppm signal belongs to a precursor of M_{412}. (In contrast, low concentrations of X persist at temperatures as high as −60 °C. This is inconsistent with the thermal behavior of L.) At −22 °C, M relaxes to LA, as observed on other occasions. However, at this temperature, a small

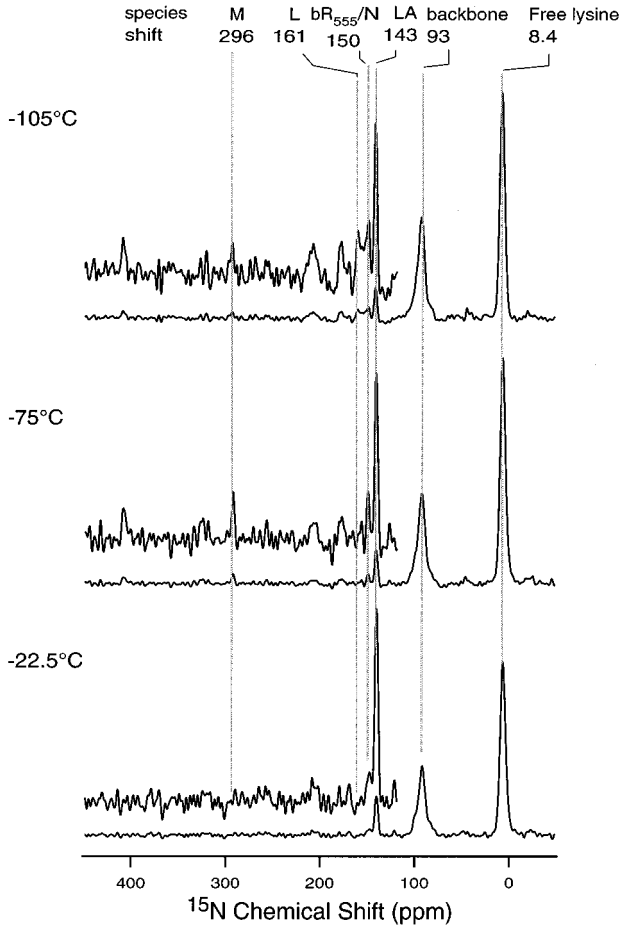

FIGURE 4: ^{15}N CP/MAS spectra of [ϵ-^{15}N]Lys-bR in 0.1 M NaCl at pH 10.0 taken at −110 °C. Top: L, M, and N intermediates prepared at −105 °C according to the procedure in Figure 3. Middle: L has converted to M after relaxation at −75 °C in the dark. Bottom: M and N have converted to LA after relaxation at −22.5 °C in the dark.

amount of N_{520} still persists, consistent with the relative stability of this intermediate at high pH.

The populations of the bR photointermediates depend on the illumination temperature (Figure 5). The L state is first observed at −90 °C and becomes more populated at lower preparation temperatures although the overall conversion of LA declines. The temperature dependence of the population of M reflects both the variation in conversion of LA and the variation in trapping of L. Analogously, the temperature dependence of the population of N reflects both the variation in conversion of LA and the variation in trapping of M.

DISCUSSION

The present work identifies the conditions required for SSNMR observation of the L intermediate of the bR photocycle. Four pieces of evidence support the assignment of the ^{15}N chemical shift at 161 ppm to the pSB of L_{550}:

(1) The 161 ppm signal corresponds to about 20% of the total SB signal under the conditions used by resonance Raman (Lohrmann & Stockburger, 1992) and FTIR (Weidlich et al., 1995) spectroscopists for stabilizing L.

(2) The 161 ppm signal gives way to the M_{412} signal in the dark under conditions where L_{550} is not stable but M_{412} is.

(3) Other species, such as X, seen at low temperatures with $\lambda > 540$ nm are reduced with $\lambda > 610$ nm, which

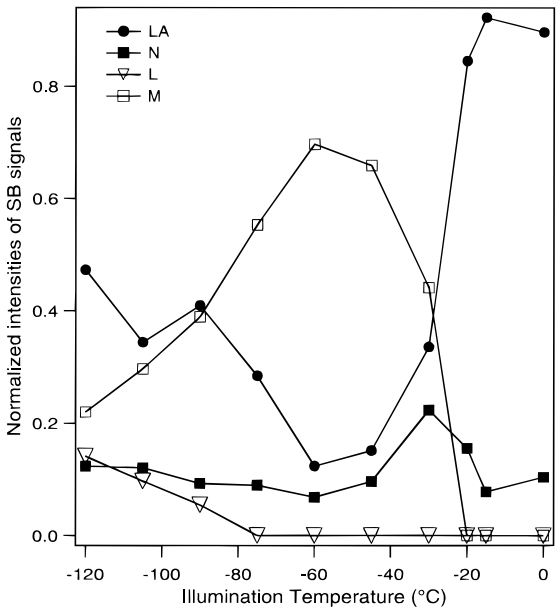

FIGURE 5: Dependence of the populations of different bR intermediates on the illumination temperature. The intensities of the SB signals were normalized against the total intensity of all the SB signals.

suggests that they result from absorption of a second photon.

(4) The observed coexistence of the 161 ppm signal with M and N signals is consistent with the equilibria between L and M, and M and N, indicated by kinetic analyses (Ames & Mathies, 1990; Varo & Lanyi, 1990, 1991a−c).

Among all the bR states, the ^{15}N signal of the SB in L, at 161 ppm, is the furthest downfield. The shielding of atoms in the polyene backbone is influenced by steric interactions and electrostatic interactions. Steric interactions cause an upfield shift by drawing electron density from the crowded proton to the attached heavy atom. Such an effect would be expected at the pSB nitrogen if the chromophore had a 13,14-*dicis* conformation. Our observation of weak shielding of the pSB nitrogen argues against a 13,14-*dicis* structure in the L state.

Electrostatic interactions affect the shielding of the pSB nitrogen (and the odd numbered carbons) by influencing the relative energies and the mixing of the pSB resonance structures shown in Figure 6. The weakest shielding of the nitrogen occurs when structure A most dominates the ground state by virtue of stabilization by a strong counterion near the pSB. Comparison with the ^{15}N chemical shifts of model compounds, particularly the 6-*s*-*trans*,13-*cis*,15-*anti* protonated Schiff bases (pSB) of retinal (Hu et al., 1995, 1997), suggests that the interaction of the pSB with its counterion is significantly stronger in L than in N_{520} (where the interaction is in turn stronger than in bR_{568}). The pSB−counterion center-to-center distance that we infer for L_{550}, from the relationship to ^{15}N chemical shifts shown in Figure 7, is 3.5 Å (as in a Cl^- salt) vs 3.68 Å for N_{520} (as in a Br^- salt) and 4.08 Å for bR_{568} (longer than in an I^- salt). These distances are qualitatively consistent with the molecular dynamics results as shown in Table 1: although the simulations of Scharnagl et al. and Schulten et al. predict different pSB−counterion distances, they both predict that the pSB moves decisively toward the nearest negative charges during the bR_{568} to L_{550} transition.

The NMR results are also consistent with FTIR observations that the pSB forms a stronger interaction with its

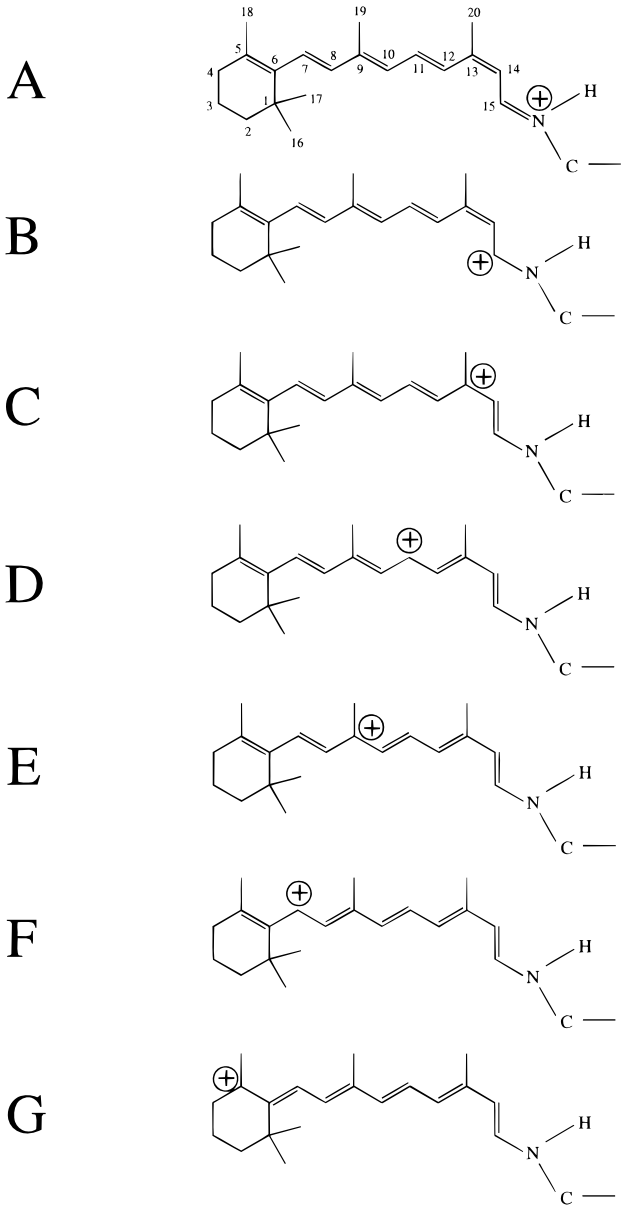

FIGURE 6: Resonance structures for protonated Schiff bases of 6-*s-trans*,13-*cis* retinal.

counterion in L than in other intermediates (Kandori et al., 1995; Maeda et al., 1991, 1992b, 1994; Yamazaki et al., 1995a, 1996), including the N_{520} intermediate formed upon reprotonation of the Schiff base (Pfefferlé et al., 1991). A strong pSB−counterion interaction in L supports models in which electrostatic interactions have a strong influence on chromophore dynamics in the early photocycle (Humphrey et al., 1995; Scharnagl et al., 1995; Zhou et al., 1993).

In addition to weak shielding of the pSB nitrogen, stabilization of resonance structure A in Figure 6 should be associated with a blue-shifted visible spectrum. This correlation between nitrogen deshielding and decreasing λ_{max} is in fact observed in model compounds and in other states of bR, as shown in Figure 8. However, for the L state, the maximum visible absorbance is at 550 nm (comparable to a bromide salt) rather than the ~491 nm expected from its ^{15}N chemical shift (comparable to a chloride salt). This anomaly suggests a strained chromophore. Distortion in the L intermediate has also been inferred from FTIR (Fahmy et al., 1989; Maeda et al., 1991; Pfefferlé et al., 1991; Weidlich et al., 1993) and resonance Raman (Lohrmann et al., 1992)

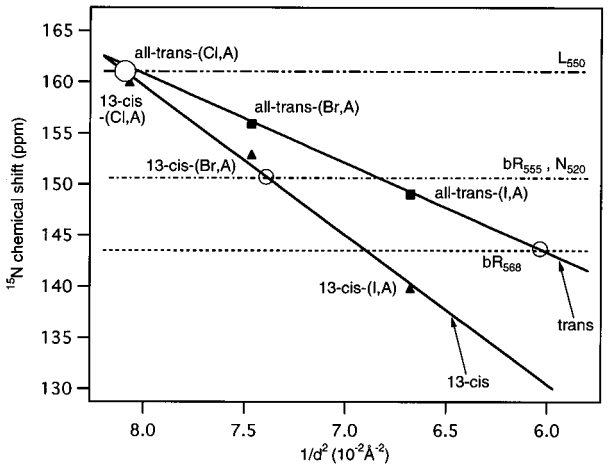

FIGURE 7: Correlation between the ^{15}N chemical shift for protonated 6-*s-trans*-retinal Schiff bases and the counterion strength measured by $1/d^2$, where d is the center−center distance between the SB nitrogen and the counterion. The filled points are the experimental data, and the solid lines show the linear least-square fits (Hu et al., 1997). The 6-*s-trans* pSB's were prepared from 13-*cis*- or *all-trans*-retinal, aniline (A), and three halides (Cl^-, Br^-, and I^-). Open circles mark the counterion strengths inferred for bR intermediates from the SB ^{15}N chemical shifts marked by the horizontal lines.

Table 1: Counterion Distances from the Schiff Base Nitrogen

		from Scharnagl et al.[a]		from Schulten et al.[a]	
intermediate	from Figure 7	closest Asp O	av distance to O's of closest Asp	closest Asp O	av distance to O's of closest Asp
bR_{568}	4.08	4.35	4.48	5.43	6.28
L	3.50	3.44	3.87	4.18	4.41
N	3.68	3.32	3.84		

[a] Personal communications.

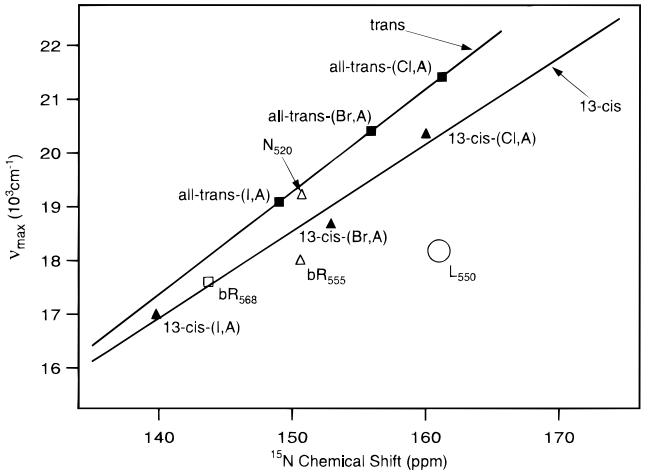

FIGURE 8: Relationship between the visible absorption maximum and the SB ^{15}N chemical shift. The notation for the model compounds is as in Figure 7. The data for bR states are labeled with their symbols. L alone deviates severely from the general relationship.

spectra, and predicted by molecular dynamics simulations (Humphrey et al., 1995; Scharnagl et al., 1994, 1995). This distortion may be due to a combination of steric interactions with neighboring residues, such as Trp182 (Maeda et al., 1992a; Yamazaki et al., 1995b) or Thr89 (Henderson et al., 1990), and the strong electrostatic interactions between the pSB and its counterion discussed above. The latter would be relieved by discharge of the SB proton in the L→M

transition. In any case, the chromophore distortion appears to be gone in the N intermediate, based on the relationship between the ^{15}N chemical shift and the visible absorption which is as expected for a relaxed chromophore. This chromophore relaxation is consistent with the orientation of the SB proton toward the cytoplasmic part of the proton pathway in the N state.

Usually distortion of a polyene is expected to involve twist about single bonds which have much lower barriers to rotation than double bonds. However, twist about the even-numbered bonds in a 6-*s*-*trans*-retinal pSB with a strong counterion would increase the energy of the excited state resonance structures in which the even-numbered bonds have more double bond character (Figure 6B−G). The result would be a blue shift of the visible spectrum to $\lambda_{max} < 491$ nm, rather than the observed red shift to $\lambda_{max} = 550$ nm. To explain a distortion-induced red shift, it is neccessary to suppose that the dominant effect is due to strain about odd-numbered bonds which have more double bond character in the ground state (Suzuki, 1969). Since the same strong pSB counterion that stabilizes the A resonance structure as the ground state will also stabilize the B resonance structure as the lowest excited state, the visible spectrum may be roughly interpreted as a measure of the energy gap between the A and B resonance structures. The observed red shift therefore specifically suggests strain around the C═N bond.

CONCLUSIONS

The L intermediate of bR has been observed by solid-state ^{15}N NMR, after illumination with $\lambda > 610$ nm, at temperatures <-90 °C, in 0.1 M NaCl at pH 7.0 and pH 10.0. At pH 10.0, L is not stable at −75 °C and relaxes to the M intermediate, consistent with the widely accepted bR photocycle. At lower temperatures, the L state is more populated, and the M state is less populated. This is also consistent with the photocycle sequence.

The 161 ppm ^{15}N chemical shift of the SB in L is significantly downfield relative to those of bR_{568} and N_{520}. This result argues against a 13,14-*dicis* conformation in L. Comparison with the chemical shifts of various retinal Schiff base salts suggests a strong interaction with the SB counterion in L. This can be reconciled with the red-shifted visible spectrum of L if there is double bond strain in the chromophore, especially around the C═N bond.

ACKNOWLEDGMENT

We thank Dr. C. Scharnagl and Dr. K. Schulten for sharing their unpublished coordinates for simulated bR photocycle intermediates.

REFERENCES

Ames, J. B., & Mathies, R. A. (1990) *Biochemistry 29*, 7181−7190.

Argade, P. V., Rothschild, K. J., Kawamoto, A. H., Herzfeld, J., & Herlihy, W. C. (1981) *Proc. Natl. Acad. Sci. U.S.A. 78*, 1643−1646.

Braiman, M. S., Mogi, T., Marti, T., Stern, L. J., Khorana, H. G., & Rothschild, K. J. (1988) *Biochemistry 27*, 8516−8520.

de Groot, H. J. M., Harbison, G. S., Herzfeld, J., & Griffin, R. G. (1989) *Biochemistry 28*, 3346−3353.

de Groot, H. J. M., Smith, S. O., Courtin, J., van der Berg, E., Winkel, C., Lugtenburg, J., Griffin, R. G., & Herzfeld, J. (1990) *Biochemistry 29*, 6873−6883.

Engels, M., Gerwert, K., & Bashford, D. (1995) *Biophys. Chem. 56*, 95−104.

Fahmy, K., Siebert, F., Grossjean, M., & Tavan, P. (1989) *J. Mol. Struct. 214*, 257−288.

Farrar, M., Lakshmi, K. V., Smith, S. O., Brown, R. S., Raap, J., Lugtenburg, J., Griffin, R. G., & Herzfeld, J. (1993) *Biophys. J. 65*, 310−315.

Fischer, W. B., Sonar, S., Marti, T., Khorana, H. G., & Rothschild, K. J. (1994) *Biochemistry 33*, 12757−12762.

Fodor, S. P. A., Pollard, W. T., Gebhard, R., van der Berg, E. M. M., Lugtenburg, J. & Mathies, R. (1988) *Biochemistry 27*, 7097−7101.

Gerwert, K., Hess, B., Soppa, J., & Oesterhelt, D. (1989) *Proc. Natl. Acad. Sci. U.S.A. 86*, 4943−4947.

Harbison, G. S., Herzfeld, J., & Griffin, R. G. (1983) *Biochemistry 22*, 1−5.

Harbison, G. S., Smith, S. O., Pardoen, J. A., Mulder, P. P. J., Lugtenburg, J., Herzfeld, J., Mathies, R., & Griffin, R. G. (1984) *Proc. Natl. Acad. Sci. U.S.A. 81*, 1706−1709.

Harbison, G. S., Smith, S. O., Pardoen, J. A., Courtin, J. M. J., Lugtenburg, J., Herzfeld, J., Mathies, R. A., & Griffin, R. G. (1985) *Biochemistry 24*, 6955 −6962.

Henderson, R., Baldwin, J. M., Ceska, T. A., Zemlin, F., Beckmann, E., & Downing, K. H. (1990) *J. Mol. Biol. 213*, 899−929.

Hu, J. G., Griffin, R. G., & Herzfeld, J. (1994) *Proc. Natl. Acad. Sci. U.S.A. 91*, 8880−8884.

Hu, J. G., Bizounok, M., Sun, B. Q., Griffin, R. G., & Herzfeld, J. (1995) *Biophys. J. 68*, A332.

Hu, J. G., Griffin, R. G., & Herzfeld, J. (1997) *J. Am. Chem. Soc.* (in press).

Humphrey, W., Xu, D., Sheves, M., & Schulten, K. (1995) *J. Phys. Chem. 99*, 14549−14560.

Kandori, H., Yamazaki, Y., Sasaki, J., Needleman, R., Lanyi, J. K., & Maeda, A. (1995) *J. Am. Chem. Soc. 117*, 2118−2119.

Khorana, H. G., Gerber, G. E., Herlihy, W. C., Gray, C. P., Anderegg, R. J., Nihei, K. F., & Biemann, K. (1979) *Proc. Natl. Acad. Sci. U.S.A. 76*, 5046−5050.

Lakshmi, K. V., Auger, M., Raap, J., Lugternburg, J., Griffin, R. G., & Herzfeld, J. (1993) *J. Am. Chem. Soc. 115*, 8515−8516.

Lakshmi, K. V., Farrar, M. R., Raap, J., Lugtenburg, J., Griffin, R. G., & Herzfeld, J. (1994) *Biochemistry 33*, 8853−8857.

Lohrmann, R., & Stockburger, M. (1992) *J. Raman Spectrosc. 23*, 575−583.

Maeda, A., Sasaki, J., Pfefferle, J. M., Shichida, Y., & Yoshizawa, T. (1991) *Photochem. Photobiol. 53*, 911−921.

Maeda, A., Sasaki, J., Ohkita, Y. J., Simpson, M., & Herzfeld, J. (1992a) *Biochemistry 31*, 12543−12545.

Maeda, A., Sasaki, J., Shichida, Y., & Yoshizawa, T. (1992b) *Biochemistry 31*, 462−467.

Maeda, A., Sasaki, J., Yamazaki, Y., Needleman, R., & Lanyi, J. K. (1994) *Biochemistry 33*, 1713−1717.

Mathies, R. A., & Li, X.-Y. (1995) *Biophys. Chem. 56*, 47−55 .

Mathies, R. A., Lin, S. W., Ames, J. B., & Pollard, W. T. (1991) *Annu. Rev. Biophys. Biophys. Chem. 20*, 491−518.

Nilsson, A., Rath, P., Olejnik, J., Coleman, M., & Rothschild, K. J. (1995) *J. Biol. Chem. 270*, 29746−29751.

Oesterhelt, D., & Stoeckenius, W. (1971) *Nature (London), New Biol. 233*, 149−152.

Oesterhelt, D., & Stoeckenius, W. (1973a) *Proc. Natl. Acad. Sci. U.S.A. 71*, 1234−1238.

Oesterhelt, D., & Stoeckenius, W. (1973b) *Proc. Natl. Acad. Sci. U.S.A. 70*, 2853−2857.

Oesterhelt, D., & Stoeckenius, W. (1974) *Methods Enzymol. 31*, 667−678.

Orlandi, G., & Schulten, K. (1979) *Chem. Phys. Lett. 64*, 370−374.

Ovchinnikov, Y. A., Abdulaev, N. G., Feigina, M. Y., Kiselev, A. V., & Lobanov, N. A. (1979) *FEBS Lett. 100*, 219−224.

Pettei, M. J., Yudd, A. P., Nakanishi, K., Henselman, R., & Stoeckenius, W. (1977) *Biochemistry 16*, 1955−1959.

Pfefferlé, J.-M., Maeda, A., Sasaki, J., & Yoshizawa, T. (1991) *Biochemistry 30*, 6548−6556.

Scharnagl, C., Hettenkofer, J., & Fischer, S. F. (1994) *Int. J. Quantum Chem. Quantum Biol. Symp. 21*, 33−56.

Scharnagl, C., Hettenkofer, J., & Fischer, S. F. (1995) *J. Phys. Chem. 99*, 7787−7800.

Schulten, K. (1978) in *Energetics and Structure of Halophilic Microorganisms* (Caplan, S., & Ginzburg, M., Eds.) pp 331−334, Elsevier, Amsterdam.

Schulten, K., & Tavan, P. (1978) *Nature 272*, 85−86.

Schulten, K., Schulten, Z., & Tavan, P. (1984) in *Information and Energy Transduction in Biological Membranes* (Bolis, L., Helmreich, E., & Passow, H., Eds.) pp 113−131, Alan R. Liss, New York.

Sonart, S., Marti, T., Rath, P., Fischer, W., Coleman, M., Nilsson, A., Khorana, H. G., & Rothschild, K. J. (1994) *J. Biol. Chem. 269*, 28851−28858.

Subramaniam, S., Gerstein, M., Oesterhelt, D., & Henderson, R. (1993) *EMBO J. 12*, 1−8.

Suzuki, H. (1967) *Electronic Absorption Spectra and Geometry of Organic Molecules: An Application of Molecular Orbital Theory*, Academic Press, New York.

Varo, G., & Lanyi, J. K. (1990) *Biochemistry 29*, 2241−2250.

Varo, G., & Lanyi, J. K. (1991a) *Biochemistry 30*, 5008−5015.

Varo, G., & Lanyi, J. K. (1991b) *Biochemistry 30*, 5016−5022.

Varo, G., & Lanyi, J. K. (1991c) *Biophys. J. 59*, 313−322.

Weidlich, O., & Siebert, F. (1993) *Appl. Spectrosc. 47*, 1394−1400.

Weidlich, O., Friedman, N., Sheves, M., & Siebert, F. (1995) *Biochemistry 34*, 13502−13510.

Yamazaki, Y., Hatanaka, M., Kandori, H., Sasaki, J., Karstens, W. F. J., Raap, J., Lugtenburg, J., Bizounok, M., Herzfeld, J., Needleman, R., Lanyi, J., & Maeda, A. (1995a) *Biochemistry 34*, 7088−7093.

Yamazaki, Y., Sasaki, J., Hatanaka, M., Kandori, H., Maeda, A., Needleman, R., Shinada, T., Yoshihara, K., Brown, L. S., & Lanyi, J. (1995b) *Biochemistry 34*, 577−582.

Yamazaki, Y., Tuzi, S., Saito, H., Kandori, H., Needleman, R., Lanyi, J., & Maeda, A. (1996) *Biochemistry 35*, 4063−4068.

Zhou, F., Windemuth, A., & Schulten, K. (1993) *Biochemistry 32*, 2291−2306.

BI970416Y